AIAA JOURNAL
Vol. 48, No. 12, December 2010

Analytical Investigation of the Toughening Potential of a Failure Tailoring Concept

Robert A. Haynes*
Georgia Institute of Technology, Atlanta, Georgia 30332
and
D. Stefan Dancila† and Erian A. Armanios‡
University of Texas at Arlington, Arlington, Texas 76019

DOI: 10.2514/1.J050547

A parametric study has been performed to determine the upper bounds of toughening benefit achievable using an approximate model for the response of one-dimensional, tailored, flexible composite-material tethers with progressive failure. The tailoring concept is achieved through judicious arrangement of redundant load paths with unequal length and strength and has been proposed, modeled, and experimentally verified in previous research. The model is recast in this work using nondimensional material-independent parameters that are varied over ranges of interest in advanced composites. The effects of each parameter on the response of the tailored member are discussed. An increase of nearly two orders of magnitude in toughness over an untailored member is found to be attainable by taking complete advantage of the energy dissipated by the failure of each load path within the bounds of the study. Challenges to implementation of the tailored member as approximated by the model are also discussed.

Nomenclature

b	=	width of the member
E_{11}	=	modulus of elasticity
F	=	nondimensional load
K	=	stiffness of a link
k	=	stiffness of a segment
L	=	length of the member
l	=	length of a segment
n	=	number of links
P	=	load
t	=	thickness of a segment
α	=	reduced secondary-segment thickness
β	=	reduced connector segment length
γ	=	toughening factor
δ	=	tip displacement
ε_f^u	=	failure strain
λ	=	reduced secondary-segment length
μ_{12}	=	shear modulus
ξ	=	nondimensional tip displacement

Subcripts

c	=	connector-segment quantities
p	=	primary-segment quantities
s	=	secondary-segment quantities

Received 28 March 2010; revision received 4 August 2010; accepted for publication 20 August 2010.

*Graduate Research Assistant, School of Aerospace Engineering, 270 Ferst Driver Northwest. Member AIAA.

†Associate Professor, Mechanical and Aerospace Engineering Department, School of Mechanical and Aerospace Engineering, Box 19018, 500 West First Street, Woolf Hall 211. Senior Member AIAA.

‡Professor and Chair, Mechanical and Aerospace Engineering Department, School of Mechanical and Aerospace Engineering, Box 19018, 500 West First Street, Woolf Hall 211. Associate Fellow AIAA.

I. Introduction

TOUGHENED structures have applications in improving crashworthiness by absorbing much of the energy associated with impact loading [1,2]. Vehicles subject to crash loading are often not subject to preservation of structural integrity, and a concept that enhances survivability of crew and payload would be considered desirable for incorporation into the structure. Inflatable structures can also benefit from materials that absorb energy through an increased resistance to pressure pulses [3].

A toughening concept based on designed failure modes capable of generating a yield-type response and increased energy dissipation in tension-loaded 1-D structures (e.g., tethers, straps, ropes, etc.) has been proposed, patented, modeled, and experimentally verified in prior work by two of the authors [4–8]. The tailoring concept employed herein relies upon the redistribution of load among a network of redundant load-path elements that have unequal length and strength. The naturally occurring distribution of strength among nominally identical structural elements induces a sequential progressive-failure process, resulting in increased fracture surface area. While not limited to composite-material construction, the failure tailoring concept can advantageously benefit from the high specific strength and stiffness that are typical of high-performance fibers and elastomeric matrices. Experimental results obtained by testing tailored composite straps under quasi-static and impulsive loading have demonstrated the functionality of the tailoring concept and its toughening benefit [8]. Models that have been developed to predict the response were verified through comparison with test data.

Significant increases in energy dissipation are achievable through appropriate selection of tailoring parameters. It is of interest to analytically investigate the toughening potential of the tailoring concept by using the developed response models. This paper presents the results of a parametric study aimed at providing insight into the upper bounds of toughening benefit and the associated tailored configurations, as well as insight into the challenges that need to be overcome for practical implementation of these configurations.

II. Tailoring Concept

The tailoring concept used here has been characterized in detail in prior work [4–8]. A brief review of the concept as it pertains to this work is provided in the following for convenience. The beneficial response is achieved through the use of axially stiff, bendwise flexible materials. A tailored member is shown in Fig. 1a, consisting

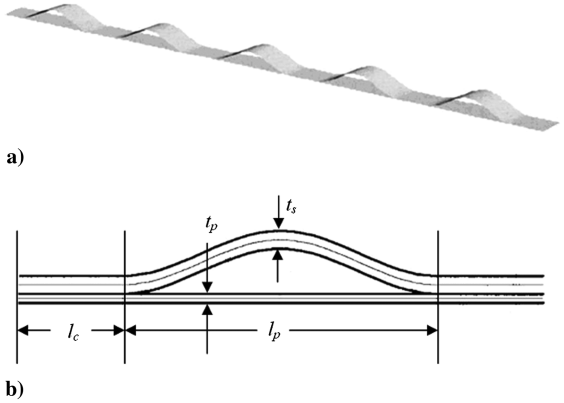

Fig. 1 Tailored member: a) five-link isometric view and b) a single link.

of five links. A continuous primary load-path spans the length of the member, while a secondary segment is attached to the primary segment at even intervals along the length of the member, creating multiple links in series. All links are identical and consist of a connector (denoted by its length l_c), where the primary and secondary segments are adhered; a region where the two segments are separate (denoted by their length l_p); and another connector, as shown in Fig. 1b. The secondary segment in each link must be longer and have a larger cross-sectional area than the primary segment to prevent failure of any secondary segments before all primary segments have failed. Load transfer between adjacent links where one primary segment has failed and the other is still intact occurs through the connector between the two adjacent links.

Upon initial tensile loading of the member, only the primary segments and the connectors carry load. Since all primary segments have ideally the same properties, their theoretical failure load will be the same. In practice, however, the failure loads will generate a distribution, causing each link to fail sequentially instead of simultaneously. Upon each failure, the member partially unloads, resulting in an advantageous loss of energy in the system.

An analytical model has been developed to characterize the response of tailored structures for a material system that is linearly elastic up to the point of failure. An example of a tailored member and its equivalent untailored counterpart is shown in Fig. 2, along with of a typical yield response under quasi-static loading. The untailored member consists of the same material system, orientation, total length, and total cross-sectional area but has no detached secondary segment. The total thickness of the member is the sum of the thicknesses of the primary segment, t_p, and the secondary segment, t_s. F and ξ are the nondimensional load and tip displacement, respectively, defined subsequently in Eqs. (12) and (13). Note that the untailored response resembles the response of a brittle material while the tailored member exhibits a yield-type response.

The 10 parameters that describe the model are reproduced and described in Table 1. It is useful to recast several of the parameters into nondimensional counterparts, also listed and defined in Table 1. The reduced parameters can be divided into two categories: those that change the relative magnitude and distance between peaks of the response curve and scaling factors that do not affect the shape of the tailored member's response. The parametric study described herein focuses only on parameters that control the response-curve shape.

III. Modeling of Response

The stiffness model is based on calculating the stiffness of the member at each stage of the loading process. This model assumes moderate loading rates and considers inertial effects within the tether to have a negligible influence on the response, due to a significantly higher wave speed in the tether as compared to the load-application rate. Therefore, linear time-independent equations are used for calculating the stiffnesses of the primary and secondary segments and connector.

Three models of varying degrees of modeling accuracy and simplicity have been introduced and will be summarized in the present work, starting with the most accurate. The accurate-connector-stiffness model takes into account changes in the stiffness of the connector as links fail; specifically, the total stiffness of the model is

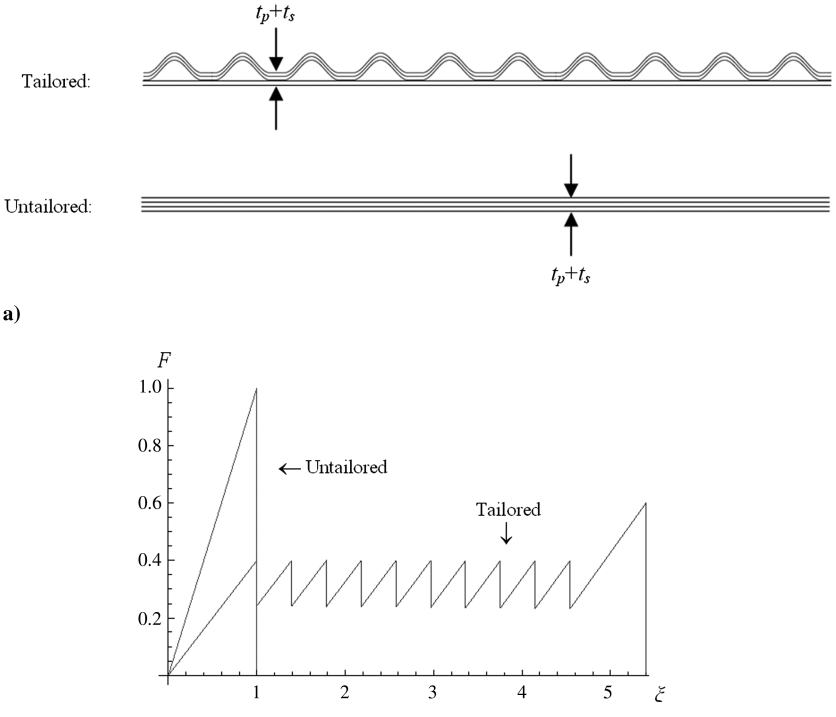

Fig. 2 Comparison of three-ply tailored and untailored members a) physical representation (note that total thickness and length in the tailored and untailored members are equal) and b) typical load-displacement curve.

Table 1 Basic configuration parameters

Parameter	Description	Reduced parameter	Definition	Effect
E_{11}	Modulus of elasticity	E_{11}	(No change)	Scaling
l_p	Length of the primary segment	l_p	(No change)	——
t_p	Thickness of the primary segment	A_p	$t_p b$	——
b	Width of the tether	(Combined with t_p to make A_p)	(No longer needed)	——
μ_{12}	Shear modulus	μ_{12}	(No change)	Shape and scaling
l_s	Length of the secondary segment	λ	l_s/l_p	——
t_s	Thickness of the secondary segment	α	t_s/t_p	——
l_c	Length of the connector	β	l_c/l_p	——
ε_f^u	Failure strain	ε_f^u	(No change)	——
n	Number of links	n	(No change)	——

$$K_i = \left(\sum_{p=1}^{n+1}\frac{1}{k_c^p} + \sum_{q=1}^{n}\frac{1}{k_l^q}\right)^{-1}, \qquad 1 \le i \le (n+1) \tag{1}$$

where the primary and secondary-segment stiffnesses are used in such a way that

$$k_l^q = \begin{cases} k_p & s_q \\ k_s & \neg s_q \end{cases} \tag{2}$$

$$k_p = E_{11} b t_p / l_p, \qquad k_s = E_{11} b t_s / l_s \tag{3}$$

where l_p, t_p, l_s, and t_s are the length and thickness of the primary and secondary segments, respectively; E_{11} and b are the modulus of elasticity of the material along the loading direction and width of the tether, respectively, as defined in Table 1; and

$$k_c^p = \begin{cases} k_c^{tp} & ((p=1) \wedge \neg s_1) \vee ((p=(n+1)) \wedge \neg s_n) \\ k_c^{ts} & ((p=1) \wedge s_1) \vee ((p=(n+1)) \wedge s_n) \\ k_c^{pp} & (2 \le p \le n) \wedge s_{p-1} \wedge s_p \\ k_c^{ps} & (2 \le p \le n) \wedge s_{p-1} \forall s_p \\ k_c^{ss} & (2 \le p \le n) \wedge \neg s_{p-1} \wedge \neg s_p \end{cases} \tag{4}$$

The connector stiffness $k_c^{(t,p,s)(p,s)}$, defined previously [7], depends on whether a primary, secondary, or terminal segment is carrying a load at each end of the connector. The terminal segment is a connector at the end of the tether. The Boolean operator s takes the value TRUE as long as the primary segment of a particular link has not yet failed. Using the stiffnesses in Eq. (4), the load developed in the tether, P, is a function of the end displacement δ, as

$$P(\delta) = \sum_{i=1}^{n+1} P_i(\delta) \tag{5}$$

where

$$P_i = \begin{cases} K_i(\delta - (i-1)(l_s - l_p)) & \delta \in (\delta_i^s, \delta_i^u] \\ 0, & \delta \notin (\delta_i^s, \delta_i^u] \end{cases}, \quad 1 \le i \le (n+1) \tag{6}$$

$$\delta_i^s = \begin{cases} 0, & i = 1 \\ \max[\delta_{i-1}^u, (i-1)(l_s - l_p)] & 1 < i \le (n+1) \end{cases} \tag{7}$$

and

$$\delta_i^u = \begin{cases} (i-1)(l_s - l_p) + (P_p/K_i), & i \ne (n+1) \\ (i-1)(l_s - l_p) + (P_s/K_i), & i = (n+1) \end{cases} \tag{8}$$

Predicting the response using this model is a stochastic process to account for the order in which each primary segment fails.

The accurate-connector-stiffness model can be greatly reduced by assuming an average value of the connector stiffness, defined as

$$k_c = 0.536[E_{11} b (t_p + t_s)/l_c] \tag{9}$$

where the 0.536 is an average of the normalized connector stiffnesses from Eq. (4), as derived in [7], which are not provided in the present work, because this model will be further simplified in the next paragraph. The stiffness of each link is then given by

$$K_i = \frac{k_p k_s k_c}{(n-i+1)k_s k_c + (i-1)k_p k_c + (n+1)k_p k_s} \tag{10}$$

Equations (3) and (5–8) still hold, resulting in the averaged-connector-stiffness model. This model no longer depends on the failure sequence.

Since the connector length is governed by the shear modulus, it is conceivable that a material could have a high enough μ_{12} such that $l_c \ll l_p$. In this case the connector can be treated as a point, and its effect vanishes, yielding

$$K_i = \frac{k_p k_s}{(n-i+1)k_s + (i-1)k_p} \tag{11}$$

which is termed the negligible-connector model, where Eqs. (3) and (5–8) still hold, and the response is independent of failure sequence. Since Eq. (11) was used to calculate the stiffnesses used in this study, for ease of calculation, the failure sequence is assumed to progress in order from link 1 to n. In summary, the three models encompass the accurate-connector-stiffness model (1–8), the averaged-connector-stiffness model (10), and the negligible-connector-stiffness model (11).

IV. Parametric Study

The negligible-connector model allows for the entire length of the member to be available for tailoring, since none of its length is required for connectors and the number of links can tend to infinity. While this is not a practical configuration, it does present a theoretical upper bound on the performance of the tailoring concept. Therefore, the negligible-connector model has been chosen as the model to be investigated in this parametric study, with stiffness given by Eq. (11).

The loading in the tailored member can be made dimensionless by the failure load of the untailored member as

$$F = P/E_{11} b (t_p + t_s) \varepsilon_f^u \tag{12}$$

which cancels the influence of modulus and area of the primary segment. A similar nondimensional tip displacement can be found as

$$\xi = \delta / L \varepsilon_f^u \tag{13}$$

Figure 2 uses the nondimensional force-displacement axes to plot the response of both the response of both tailored and untailored members. Note that the failure of the untailored member occurs at point $(F, \xi) = (1, 1)$. Using nondimensional parameters generalizes the effects of the physical relationship between the primary and secondary segments to tailored members of any material.

Of the reduced parameters that govern the shape of the response as provided in Table 1, the shear modulus μ_{12} is not used in the negligible-connector model, and the reduced connector length β tends to zero with negligible-connector length. Therefore, only four

shape parameters remain in the model: the reduced secondary-segment thickness and length, α and λ; the number of links n; and the failure strain of the chosen material, ε_f^u. These parameters form the basis of the parametric study. The parameters were varied over ranges of interest for advanced composite materials. Necessarily, $\alpha > 1$ to ensure the integrity of all secondary segments before failure of all primary segments, $\lambda > 1$ for load to be generated in the primary segments before the secondary segments, and n must be a positive integer. The lower bounds for α and λ would be material-dependent. To ensure that the primary segment would fail before the secondary segment starts carrying load, the following is placed as a restriction:

$$(l_s - l_p) > l_p \varepsilon_f^u \Rightarrow \lambda > \varepsilon_f^u + 1 \tag{14}$$

The reduced secondary-segment thickness α was varied over the range 1.1 to 3.0, meaning the secondary segment was at least 1.1 times as thick as the primary segment, but no more than 3 times as thick. The reduced secondary-segment length λ was varied over the range 1.04 to 10, meaning the secondary segment was at least 1.04 times as long as the primary segment, but no more than 10 times as long. The number of links n was varied over the range of 2 to 200. These upper bounds were chosen either because they are representative of limiting cases or a reasonable limit of physical properties. A failure strain of $\varepsilon_f^u = 0.04$, typical of glass fibers, was the basis for ε_f^u being varied over the range 0.01 to 0.1.

Energy dissipation is equivalent to toughness and is found by calculating the area underneath the response curve. The toughening factor γ was calculated based on the total energy dissipated by the tailored member divided by the total energy dissipated by its untailored counterpart, 0.5, as seen in Fig. 2. The toughening factor was adjusted by the ratio $(1 + \alpha)/(1 + \alpha\lambda)$ to account for increases in total volume of material used due to the increase in the number, length, and area of secondary segments. The goal of this study is to investigate the improvement in toughness associated with implementation of the tailoring concept.

Because there are four governing parameters, six three-dimensional surface plots are necessary to show the toughening factor γ that is achievable with every combination of two parameters. Even though some of these figures will cross-plot the data, each combination provides a useful perspective into the response that is not easy to identify from other plots. Figure 3 plots γ as a function of reduced secondary-segment thickness α and length λ for lower, middle, and upper values of the number of links n and the failure strain ε_f^u. Figure 4 plots γ as a function of α and n for lower, middle, and upper values of λ and ε_f^u. Figure 5 plots γ as a function of α and ε_f^u for lower, middle, and upper values of λ and n. Figure 6 plots γ as a function of λ and n for lower, middle, and upper values of α and ε_f^u. Figure 7 plots γ as a function of λ and ε_f^u for lower, middle, and upper values of α and n. Figure 8 plots γ as a function of n and ε_f^u for lower, middle, and upper values of α and λ.

The toughening factor γ has an inverse relationship with reduced secondary-segment thickness α, seen most clearly in Figs. 3b, 4g, and 5b. Therefore, a value of α as close to 1 as possible is desirable to produce the greatest toughening benefit. In practice, the lower bound for α would be material-dependent, and chosen to ensure that all secondary segments remain intact to preserve the integrity of the member until all primary segments have failed. Similarly, γ has an inverse relationship with the failure strain ε_f^u, most easily seen in Figs. 5h, 7g, and 8a. Therefore, a value of ε_f^u as low as possible is desirable to produce the greatest toughening benefit. In practice, the value of ε_f^u would be determined by the chosen material system.

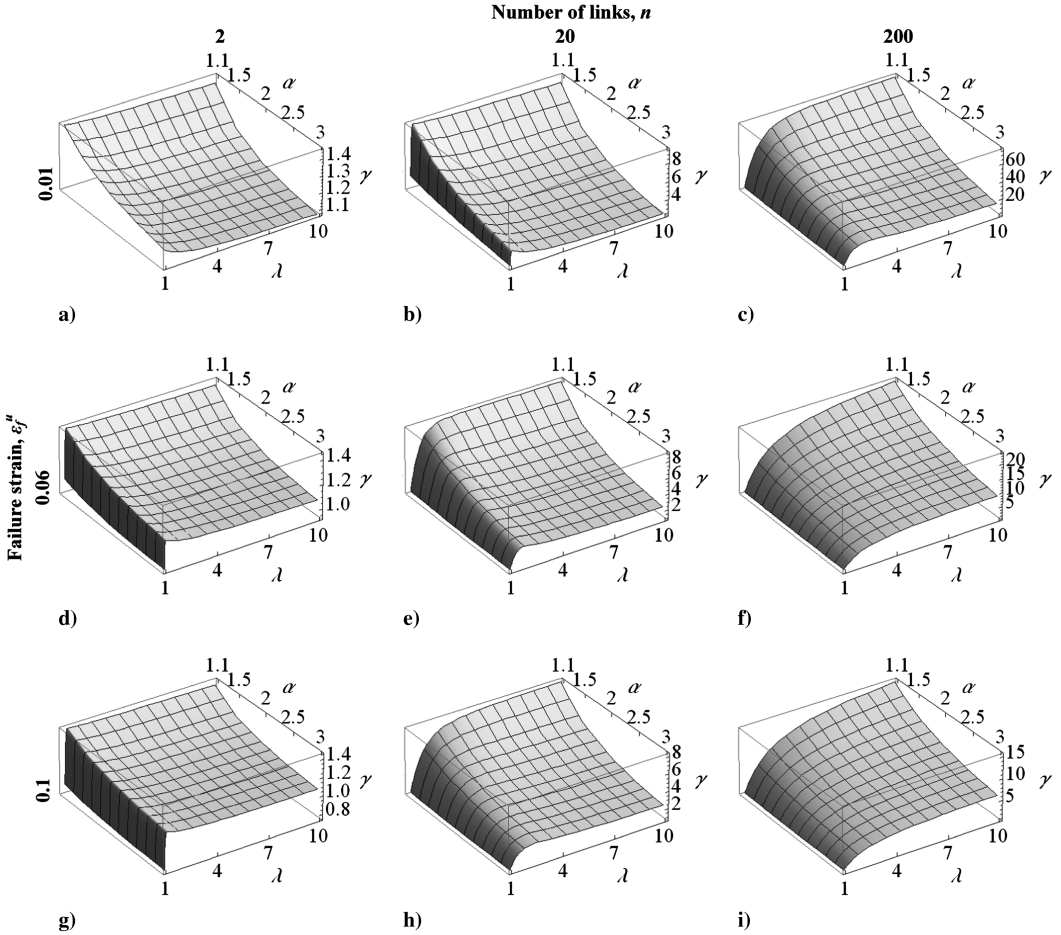

Fig. 3 Toughening factor γ as a function of reduced secondary-segment thickness α and length λ for low, middle, and high values of the number of links n and failure strain ε_f^u.

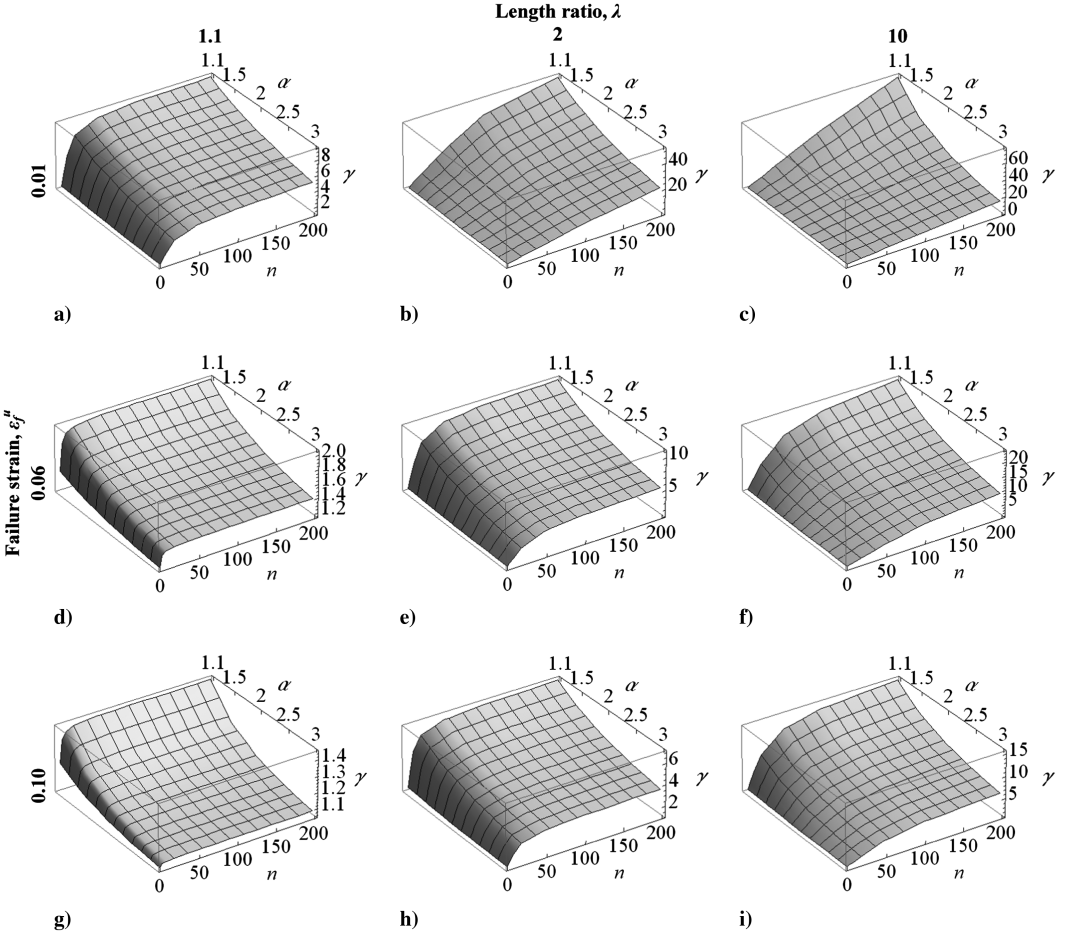

Fig. 4 Toughening factor γ as a function of reduced secondary-segment thickness α and the number of links n for low, middle, and high values of reduced secondary-segment length λ and failure strain ε_f^u.

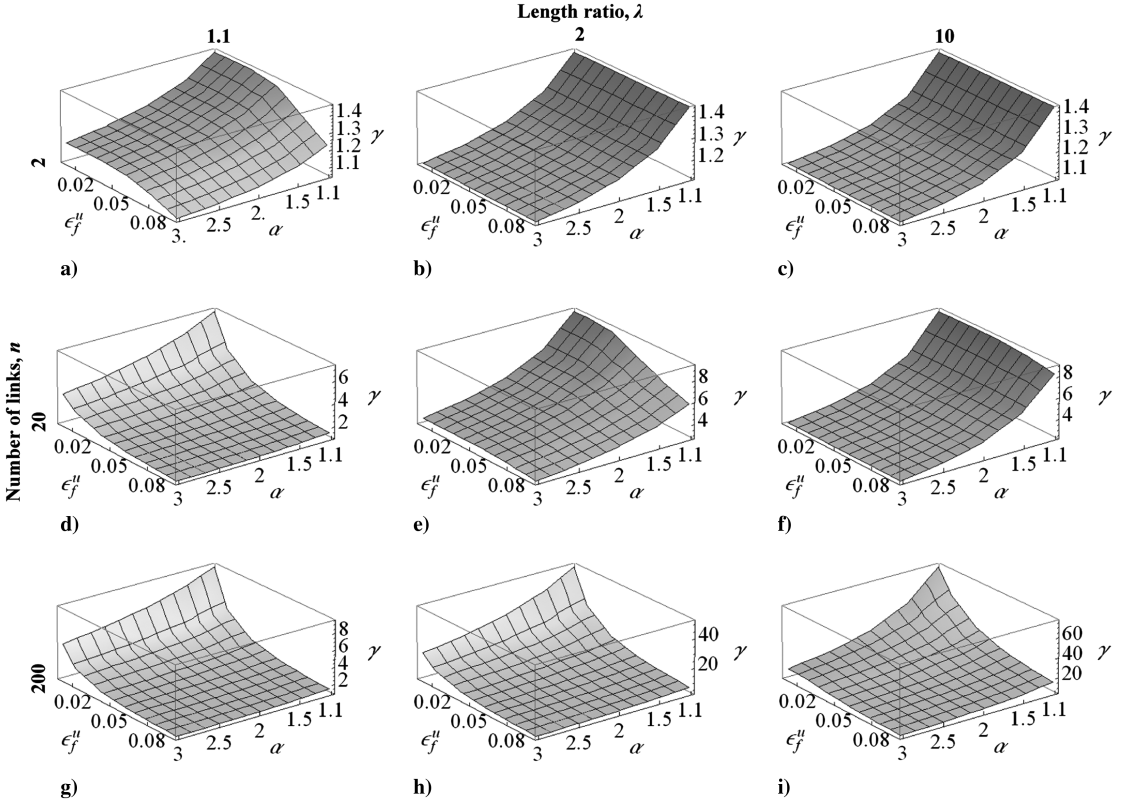

Fig. 5 Toughening factor γ as a function of reduced secondary-segment thickness α and failure strain ε_f^u for low, middle, and high values of reduced secondary-segment length λ and the number of links n.

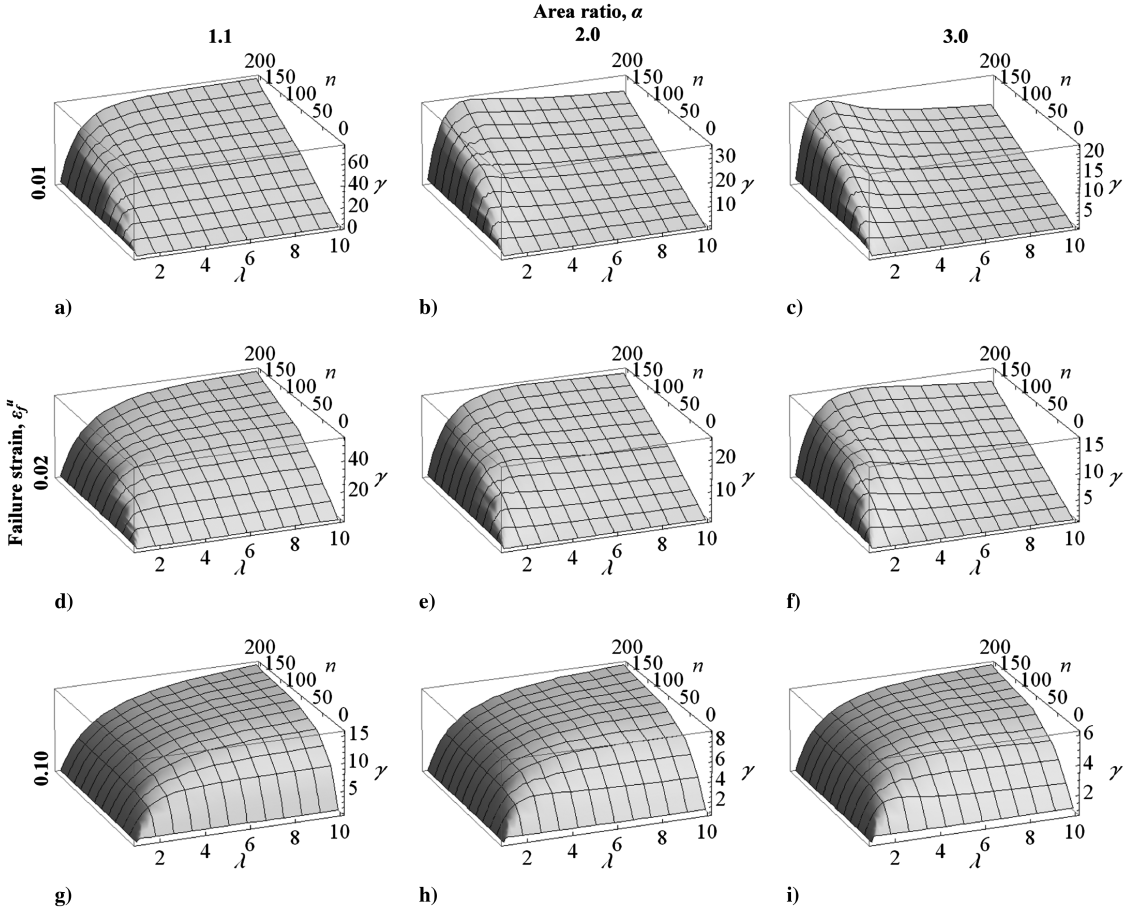

Fig. 6 Toughening factor γ as a function of reduced secondary-segment length λ and the number of links n for low, middle, and high values of reduced secondary-segment thickness α and failure strain ε_f^u.

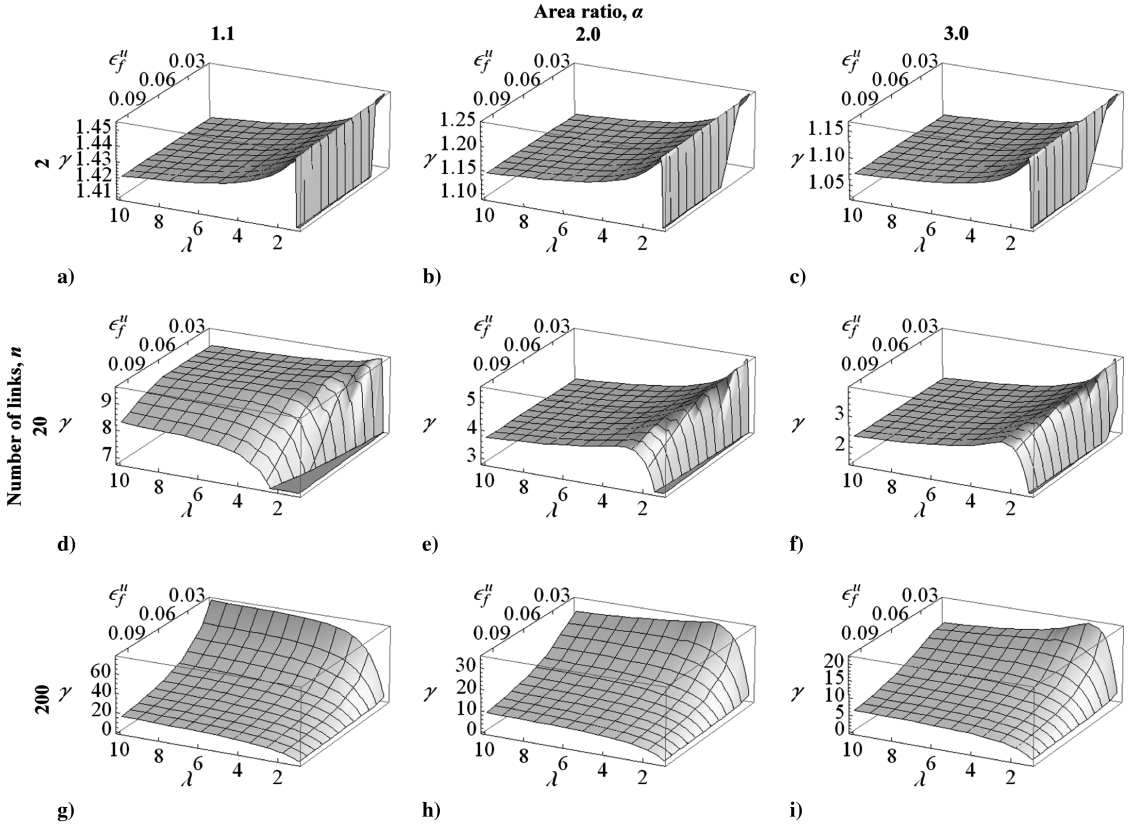

Fig. 7 Toughening factor γ as a function of reduced secondary-segment length λ and failure strain ε_f^u for low, middle, and high values of reduced secondary-segment thickness α and number of links n.

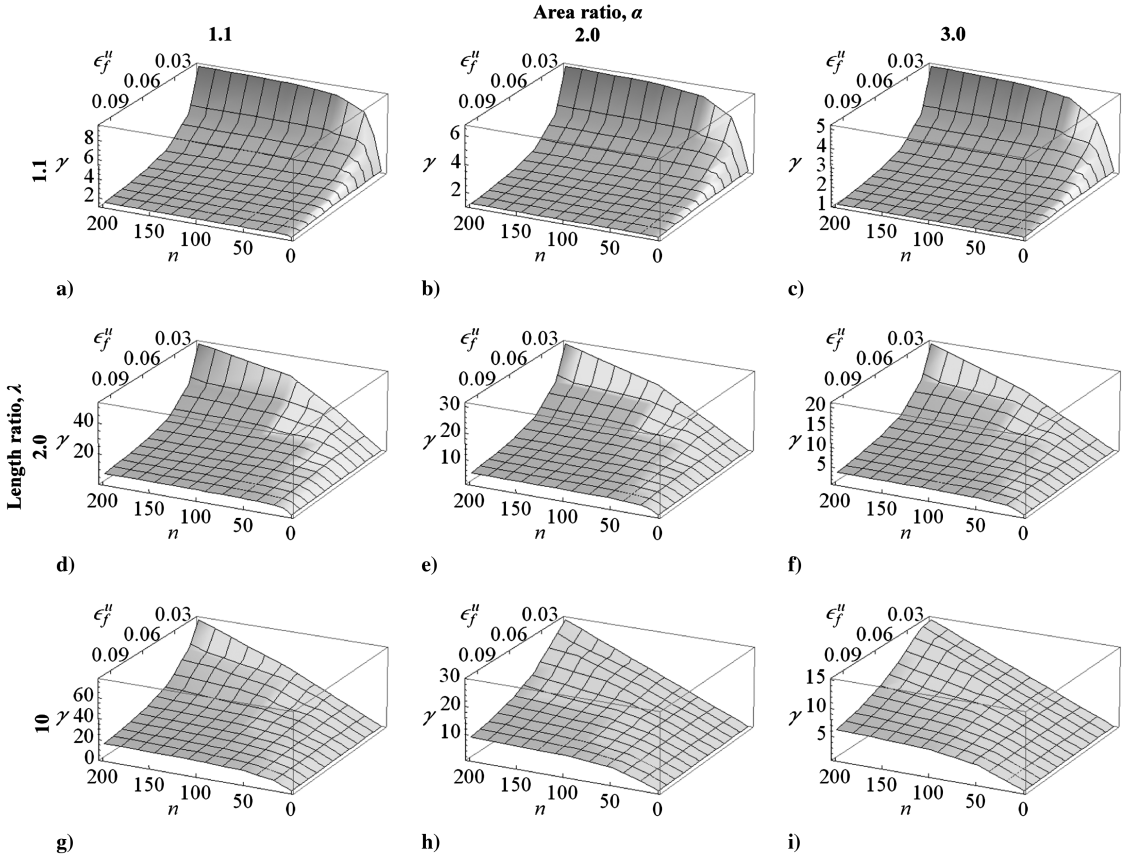

Fig. 8 Toughening factor γ as a function of the number of links n and failure strain ε_f^u for low, middle, and high values of reduced secondary-segment thickness α and length λ.

The number of links n has a direct relationship to the toughening factor γ, which is most apparent in Figs. 4c, 6a, and 8i. This suggests it is desirable to include as many links as possible into a tailored member. A practical upper limit on n will be governed by the length of the tether available for tailoring and the manufacturing process's ability to produce smaller links. Recall that the model used for this study assumes an infinitesimal connector length l_c, but in reality, l_c will be finite, and the length of the tether available for tailoring will be

$$nl_p = L - l_c(n+1) \tag{15}$$

where l_p is the length of the primary segment and L is the total length of the member. Therefore, the maximum n will be

$$n_{\max} = \frac{L - l_c}{l_p + l_c} \tag{16}$$

Since L, l_p, and l_c must be non-negative, to increase γ, one can increase L, decrease l_c, or decrease l_p. The total length of the tether, L, will depend on the application; the smallest that l_c can be made will depend on the material's ability to transfer shear stresses between the primary and secondary segments of adjacent links; the lower bound for l_p is governed by the manufacturing process. However, the caveat is that for large n, the gains in toughening potential begins to diminish, as can be seen in Figs. 4i, 6g, and 8g. It appears from these figures that there is a practical limit to the toughening factor γ obtainable by increasing n. While not bounded, increases in large values of n produce only small increases in γ.

The toughening factor γ has an optimal value that corresponds to a finite value of reduced secondary-segment length λ for a given, α, n, and ε_f^u, as seen in Figs. 3d, 6c, and 7f. For example, take Fig. 6c, where $\alpha = 3.0$ and $\varepsilon_f^u = 0.01$; for 200 links ($n = 200$), there is an apparent maximum toughening factor of $\gamma \cong 20$ corresponding to a reduced secondary-segment length of $\lambda \cong 2$. For $\lambda < 2$, there is a sharp decrease in γ for decreasing λ, but for $\lambda > 2$, γ decreases with increasing λ, although less sharply. The reason for this maximum is due to the correction factor, $(1+\alpha)/(1+\alpha\lambda)$, that is applied to γ, as mentioned previously. Therefore, the greatest toughening benefit will be achieved for a λ that depends on the reduced secondary-segment thickness α, the number of links n, and the failure strain ε_f^u.

Figure 9 shows the normalized force-displacement responses of both a tailored and untailored member as each of the four parameters of interest in this parametric study are varied. Initial values for the four parameters were chosen pseudorandomly, but in such a way as to demonstrate important trends. Specifically, the reduced secondary-segment thickness and length, α and λ, the initial number of links n, and the failure strain ε_f^u were initially chosen to be 2.5, 1.15, 10, and 0.04, respectively. Also displayed on each subplot is the toughening factor γ, which has a value of 2.14 for the initial values of the parameters.

First, Figs. 9a and 9b show the effect of decreasing α from 2.5 to 1.5 on the normalized force-displacement response. A corresponding 30% increase in the toughening factor is achieved with this decrease in α, as now $\gamma = 2.78$. Physically, the effect of decreasing α is to make the primary segments stronger relative to the secondary segments, which increases the energy dissipated with the failure of a primary segment.

Second, Figs. 9b and 9c show how increasing the number of links n from 10 to 20 changes the normalized force-displacement response. The extra links mean the tether unloads about 20% less after each failure, calculated as ~40% unloading for $n = 10$ and ~20% unloading for $n = 20$. A 9.4% increase in γ is associated with this increase in n, as γ increases to 3.04.

Third, Figs. 9c and 9d show how the normalized force-displacement response changes when the failure strain ε_f^u is decreased from 0.04 to 0.01. A corresponding 129% increase in γ is achieved with this decrease in ε_f^u, as now $\gamma = 6.97$. Note the 231% increase in nondimensional tip displacement (from 4.9 to 16.2). However, this does not correspond to an increase in the actual tip displacement; by using Eq. (13), it can be shown that there is in fact a

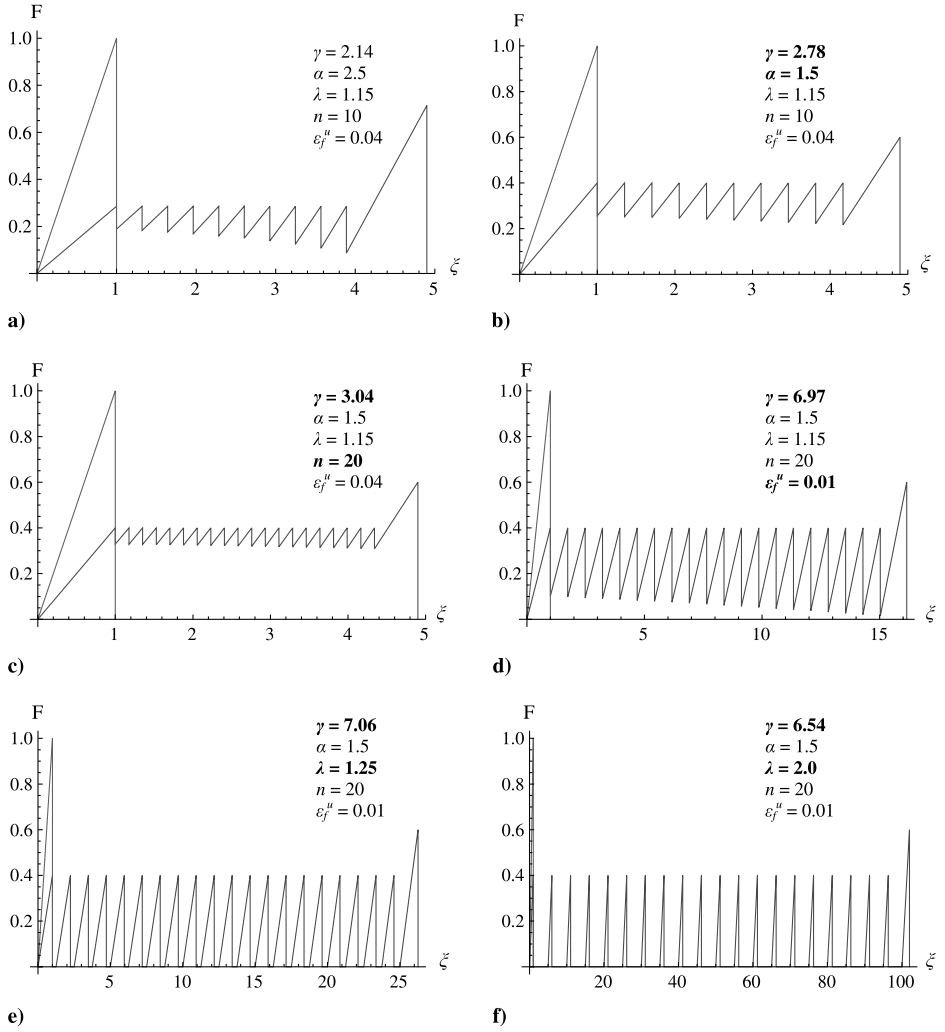

Fig. 9 Comparison of a typical response curve for a) reduced secondary-segment thickness $\alpha = 2.5$, number of links $n = 10$, reduced secondary-segment length $\lambda = 1.15$, and failure strain $\varepsilon_f^u = 0.04$, including toughening factor γ; b) decreasing α to 1.5; c) increasing n to 20; d) decreasing ε_f^u to 0.01; e) increasing λ to 1.25; and f) increasing λ to 2.0. Bold corresponds to changes from the previous subplot.

17% decrease in the actual tip displacement, δ (from $0.196L$ to $0.162L$). Physically, decreasing the failure strain is equivalent to using a stiffer material, which in an untailored tether would dissipate less energy, because the area under the force-displacement curve would be lower. However, since the force-displacement response is normalized by the untailored response, the tailored response performs much better. This suggests that the tailoring concept investigated in this work is ideally suited for use with brittle materials.

Fourth, the effect on the normalized force-displacement response of increasing the reduced secondary-segment length λ from 1.15 to 1.25 to 2.0 is shown in Figs. 9d–9f, respectively. By increasing λ from 1.15 to 1.25, the toughening factor γ increases from 6.97 to 7.06, a 1.3% increase, and by increasing λ from 1.25 to 2.0, γ decreases from 7.06 to 6.54: a 7.4% decrease. Note that the highest γ occurs when failure of a primary segment allows the tailored member to completely unload and any further increase in tip displacement causes the tailored member to start carrying load again. This follows from a physical standpoint, because failure of each primary segment will dissipate all of the strain energy. However, further increases in λ require more material without dissipating more energy, resulting in a lower toughening factor.

V. Optimization Study

To confirm the findings of the parametric study, a constrained optimization study was conducted with the goal of reaching a maximum toughness factor γ over the parameter value ranges used in the parametric study. Random values were selected for the number of links n, because it must be a positive integer. The optimization is computationally expensive for higher values of n; therefore, only 10 random values were selected in addition to $n = 2$ and $n = 200$, which were the upper and lower bounds of n from the parametric study. The optimization of the remaining parameters (namely, the reduced secondary-segment thickness and length, α and λ, and the failure strain of the chosen material, ε_f^u) was conducted using a numerical global maximizer in Mathematica [9], with inputs of the toughening-factor function and the ranges of interest as used in the parametric study: namely, $\{1.1 < \alpha < 3\}$, $\{1.04 < \lambda < 10\}$, and $\{0.01 < \varepsilon_f^u < 0.1\}$.

Table 2 presents the optimized parameters, sorted by the number of links n and the corresponding toughening factor γ. For all n, the values of the reduced secondary-segment thickness α and failure strain ε_f^u that produce maximum γ were 1.1 and 0.01, respectively, which correspond to the lowest value used in the parametric study and agree with the trends seen in the parametric study. The optimal value of the reduced secondary-segment length λ increased with increased n. The combination of n and λ that produced the greatest toughening benefit was $n = 200$, its upper bound from the parametric study, and $\lambda = 4.54$. These optimized parameters (namely, $\alpha = 1.1$, $\lambda = 4.54$, $n = 200$, and $\varepsilon_f^u = 0.01$) produced a toughening factor of $\gamma = 71.4$, indicating that the a tailored member with these parameters can dissipate up to 71.4 times the energy of its equivalent untailored counterpart. This represents a significant

Table 2 Results of optimization study

n	α	ε_f^u	λ	γ
2	1.1	0.01	1.04	1.45
4	1.1	0.01	1.05	2.81
16	1.1	0.01	1.18	7.76
36	1.1	0.01	1.40	16.6
37	1.1	0.01	1.40	16.9
67	1.1	0.01	1.84	29.5
91	1.1	0.01	2.23	38.7
102	1.1	0.01	2.42	42.7
144	1.1	0.01	3.26	56.4
155	1.1	0.01	3.5	59.6
196	1.1	0.01	4.44	70.5
200	1.1	0.01	4.54	71.4

increase in energy dissipation capability, and elucidates the potential of the tailoring concept investigated in this work.

VI. Challenges to Implementation

It is worth reiterating the physical limitations on the theory used and on each of the parameters investigated in this study. As mentioned earlier, the model chosen produces the maximum possible energy dissipation by assuming a transfer of load at the connector over an infinitesimal area. When the first primary segment fails, the load must be transferred through the connectors to the adjoining secondary segments. In practical implementation, the connector will have a finite length, which cannot be neglected and will depend on the properties of material system used.

Failure of the primary segment will change the stiffness of the connector. As a result, the failure sequence of the tailored member will influence its response. Therefore, dissipating as much energy as suggested by this study is subject to confirmation using a more accurate stiffness model. This will be the subject of a subsequent publication. The purpose of the current investigation is simply to provide a theoretical evaluation of the maximum toughening potential achievable using this tailoring concept.

As for each of the parameters, theoretically, any reduced secondary-segment thickness greater than one, i.e., $\alpha > 1$, will prevent failure of any secondary segment until all primary segments have failed, but in reality manufacturing errors will require $\alpha > 1 + e$, where e is a safety margin put in place to account for natural variability in the strength of the material. In this study, $e = 0.1$ was chosen arbitrarily. The failure strain ε_f^u will also be dictated by choice of material system, and could possibly be outside the range used in this study, which was $0.01 < \varepsilon_f^u < 0.1$. The reduced secondary-segment length λ and the number of links n will be dictated by the application, material system, and manufacturing process, as mentioned in the previous paragraph.

For a given application and material system, which will determine the total length of the tailored member L and the connector length l_c, respectively, Eq. (15) shows that the number of links n can still be increased indefinitely if the length of the primary segment, l_p, is made short enough. A lower bound on l_p will be dictated by the limitations of the manufacturing process, which in turn will dictate the upper bound on n. Similarly, an upper bound on the reduced secondary-segment length λ will depend primarily on the ability of the manufacturing process to produce increasingly shorter links. There is also a space consideration, which states that there must be room for the secondary segment to fit while the primary segment in the same link is still intact; an increasingly long secondary segment will take up room that could be used for other load-bearing members. One idea for achieving a high toughening benefit is to implement this tailoring concept in high-performance fibers. The extremely high aspect ratios achievable in fibers, such as carbon and glass fibers, are ideal for creating many links. Manufacture of fibers tailored in this way will require new processes.

VII. Conclusions

A parametric study has been performed on a failure tailoring concept designed to trade structural strength for toughness. The concept has been reduced to its simplest form, which produces the greatest theoretical toughening benefit, thus allowing an investigation of the upper bound of the potential of the tailoring concept. The results of the parametric study show that to achieve the greatest toughening factor γ, the reduced secondary-segment thickness α should be made as small as possible but, necessarily, greater than 1. Lower values of failure strain ε_f^u and a greater number of links n also increase γ. For given values of α, n, and ε_f^u, there is a finite optimal value of the reduced secondary-segment length λ that corresponds to a maximum γ. Implementation of this concept into high-performance fibers will require a unique manufacturing process.

Acknowledgments

The authors gratefully acknowledge the support given by the National Defense Science and Engineering Graduate Fellowship and the University of Texas System STARS Program.

References

[1] Jones, N., and Wierzbicki, T. (eds.), *Structural Crashworthiness and Failure*, Taylor & Francis, Abingdon, England, U.K., 1993, Chap. 6.

[2] Dancila, D. S., and Armanios, E. A., "Crew/Payload Crash Protection by Using Energy-Dissipating Tensile Composite Members with Progressive Failure," *Proceedings of the American Helicopter Society National Technical Specialists' Meeting on Rotorcraft Crashworthiness*, AHS International, Alexandria, VA, Sept. 1998.

[3] Dancila, D. S., "Pressure Pulse Tolerant Inflatable Space Structures," *Inflatable Space Structures Forum, 41st AIAA/ASME/ASCE/AHS/ASC Structures, Structural Dynamics and Materials (SDM) Conference*, Atlanta, GA, April 2000.

[4] Dancila, D. S., and Armanios, E. A., "Energy Absorbing Composite Members with Controlled Progressive Failure," *ASTM Sixth Symposium on Composites: Fatigue and Fracture*, ASTM International, West Conshohocken, PA, May 1995.

[5] Dancila, D. S., "Energy-Dissipating Tensile Composite Members with Progressive Failure," Ph.D. Thesis, School of Aerospace Engineering, Georgia Inst. of Technology, Atlanta, GA, March 1998.

[6] D. S. Dancila and E. A. Armanios, "Energy Dissipating Composite Members with Progressive Failure," U.S. Patent No. 6,136,406, 24 Oct. 2000.

[7] Dancila, D. S., and Armanios, E. A., "Energy Dissipating Composite Members with Progressive Failure—Concept Development and Analytical Modeling," *AIAA Journal*, Vol. 40, No. 10, 2002, pp. 2096–2104.
doi:10.2514/2.1544

[8] Dancila, D. S., and Armanios, E. A., "Energy Dissipating Composite Members with Progressive Failure: Impulsive Response and Experimental Verification," *AIAA Journal*, Vol. 48, No. 4, 2010, pp. 728–737.
doi:10.2514/1.39786

[9] Mathematica, Software Package, Ver. 6.0, Wolfram Research, Champaign, IL, 2007.

M. Hyer
Associate Editor